HUNTINGTON MEDICAL RESEARCH INSTITUTES
NEURAL ENGINEERING LABORATORY
734 Fairmount Avenue
Pasadena, California 91105

Contract No. N01-NS-1-2340
Quarterly Progress Report
Jan 1-March 31 2002
Report No. 2

"Functional Microstimulation of the Lumbosacral Spinal Cord"

Douglas McCreery, Ph. D.
Albert Lossinsky, Ph.D.
Victor Pikov, Ph.D
Leo Bullara, B.A.
William Agnew, Ph.D.

ABSTRACT

The objective of this project is to develop neuroprostheses that will allow patients with severe spinal cord injuries to regain control of their bladder and bowel. The approach is based on an array of microelectrodes that is implanted into the sacral spinal cord.

During the past quarter, three arrays of microelectrodes were implanted. One array each of 9 activated iridium microelectrodes was implanted into the S_2 levels of the sacral spinal cord of cats SP130 and SP132. The total left-to-right span of the array was 1 mm in cat SP130 and 1.6 mm in cat SP132. A silicon-substrate array of 12 electrodes sites on 4 shanks was implanted chronically into cat SP131 using the same introducer tool with a modified barrel.

Urodynamic measurements were obtained from cat Sp130 at 41 days, and from cat SP131 at 23 days after implanting the arrays. In both cats, an elevation in bladder pressure and relaxation of the urethral sphincter, and also micturition, could be elicited by pulsing with selected electrodes. In cat sp130, the greatest rise in bladder pressure was elicited from the microelectrodes whose tips were in the intermediolateral cell column (ILC). It is interesting that the electrodes in the ILC induced at least as much inhibition of the sphincter as did those closer to the cord's midline. The greatest elevation in bladder pressure was elicited when the baseline bladder pressure was low (10-20 mm Hg). When the bladder baseline pressure was higher (e.g, 20 mm Hg), the microelectrodes located in the intermediate horn induced a reduction in bladder pressure as well as suppression of spontaneous bladder contractions.

For chronic stimulation (SP130), the cat was lightly anesthetized with Propofol and we used stimulus parameters which had induced relaxation of the urethral sphincter during the urodynamic measurements Six electrodes were pulsed for a total of 24 hours (12 hrs/day) on two successive days. The stimulus waveform was cathodic-first, controlled-current, charge-balanced (biphasic) pulse pairs, 100 ΅A in amplitude and 400 ΅s in duration, at 20 Hz. The charge per phase was 40 nC, the charge density was 2,000 ΅C/cm². The pulse frequency was 20 Hz with a 10% duty cycle (1 minute of stimulation; 9 minutes without stimulation repeated indefinitely). Six of the 9 electrodes were pulsed. At the end of the 2nd day, the cat was deeply anesthetized and perfused with fixative for histologic evaluation of the electrode sites. The tissue sections were stained with Nissl stain or for the specific neuronal nuclear protein NeuN or with Fluor-Jade B, a fluorescent cytochemical marker for degenerating cells .

Collectively, the three stains (Nissl, NeuN, Fluoro-Jade B) showed viable neurons 50 - 100 ΅m away from the tips of all of the pulsed electrodes, with the exception of electrode #9, which had been subjected to rather prolonged stimulation at high amplitude (40 nC/phase) and high frequency (up to 40 Hz), 12 days prior to the time that the animal was perfused. This tip site was surrounded by a dense aggregate of inflammatory cells approximately 1175-200 ΅m in diameter, containing no recognizable neurons. Neurons surrounding the lesion did not fluoresce with the Fluoro-Jade B stain, indicating that they were not degenerating. Neurons within approximately 200 ΅m of the pulsed and unpulsed electrodes stained less darkly for NeuN, and this indicates that their metabolism had been altered by the implantation and/ or the continued presence of the array. However, the Nissl and Fluoro-Jade B stains revealed viable neurons close to all of the electrode tips, and the absence of any Fluoro-Jade B fluorescence indicated that none of these neurons was degenerating. Overall, there was no discernable difference between the pulsed and unpulsed tip sites, with the exception of electrode 9, as noted above.

METHODS

The objective of this project is to develop neuroprostheses that will allow patients with severe spinal cord injuries to regain control of their bladder and bowel. The system is based on an array of microelectrodes that is implanted into the sacral spinal cord. The procedures and hardware are being developed in cats with intact spinal cords, and in the 2nd year of the project, the implanted cats will undergo transection of the spinal cord at the low thoracic level.

Fabrication and implantation of the arrays

The arrays of 9 iridium microelectrodes extend from a epoxy superstructure. The 3 microelectrodes comprising the middle row are 1.4 mm in length. In cats SP134 and 135, the electrodes in the outboard rows were 1.5 mm in length, while in cats SP137 and SP138, they were 1.8 mm in length. The middle and outboard rows were separated by 0.8 mm, and the electrodes in each row (rostral-caudal separation) was 0.5 mm

The sacral cord was exposed using a standard dorsal laminectomy. To locate the junction of the S_1 and S_2 segments, we stimulated the perigenital skin, and recorded at each of several locations along the dorsal surface of the sacral cord. The arrays were implanted near the maximum of the 2nd component of the evoked response (the dorsal cord potential). At autopsy, the position of the array was validated by complete dissection of the spinal roots.

Our contract's work scope also includes the development of a 16-site microstimulation array based on multisite silicon substrate probes. Figure 2A shows a probe that was designed for our program by Jamile Hetke at the University of Michigan. Figure 2B shows a completed array containing two probes (total of 12 electrodes sites) extending from an epoxy superstructure. One array was implanted into the sacral cord of cat SP136.

All of the arrays were inserted with the high-speed inserter tool at a velocity of approximately 1 m/sec. The dura was then closed over the array, using 5 pre-installed sutures.

Histologic Procedures

The cats were deeply anesthetized with pentobarbital, given i.v. heparin and perfused through the aorta for 3 minutes with a prewash solution consisting of 900 ml of phosphate-buffered saline, and 0.05% procaine HCl. This was followed by a fixative containing 4% formalin and 0.25% glutaraldehyde in 0.1 M sodium phosphate buffer. Tissue blocks containing both the microelectrodes and areas rostral and caudal to the electrodes were washed overnight in 4% formalin, then in distilled water for 2 hrs, dehydrated in a graded series of ethanol and embedded in paraffin. The paraffin-embedded tissue blocks were cut at a thickness of 6-7 ：m and were picked up on histogrip-coated-slides (4 sections per slide). These slides were routed either for routine histologic staining with Nissl, or for immunohistochemistry (NeuN).

NeuN Immunohistochemistry. We performed immunohistochemistry for NeuN, on tissue sections containing either the electrode tips, or sections 8-32 ：m caudal or rostral to the electrode tips. This antibody recognizes many vertebrate neuron-specific proteins within the nuclei (primarily) and neuronal cytosol (to a slightly lesser degree) within the CNS of humans,

rats, mice, chickens, ferrets and salamanders. The mouse has been extensively studied and positive staining occurs in neuronal populations in the cerebellum, cerebral cortex, hippocampus, thalamus, spinal cord and neurons in the peripheral nervous system including dorsal root ganglia, sympathetic chain ganglia and enteric ganglia. Unreactive cell types include Purkinje, mitral and photoreceptor cells.

NeuN Labeling. Sections were deparaffinized, rehydraded in a decreasing ethanol series and washed in PBS. We employed an antigen retrieval technique in which the sections on glass slides were microwaved for 12 minutes at 70% power in acidic citrate buffer, 3 sessions at 4 min each, adding acid citrate buffer as needed. After cooling, tissue sections were rinsed 3 X in distilled H_2O, then changed to PBS buffer for a 5 min rinse, quenched with 0.1M NH_4Cl for 10 min to remove unbound aldehyde groups, rinsed in PBS 5 min and treated with 1% H_2O_2-Methanol-PBS mixture for 30 minutes to remove endogenous peroxidase activity. All incubations were carried out in a humidifying chamber (plastic container with wet paper towels and lid) at 25°C. The sections were then rinsed 5 min in PBS and blocked with PBS containing 50% goat serum for 1 hr at 25°C. After blotting, the sections were reacted with anti-NeuN antibody diluted 1:50 in PBSS (PBS containing 10% goat serum). After thorough washing with PBS (wash bottle rinse for 30 seconds), the tissue sections were incubated with a secondary antibody consisting of 1:50 dilution (in PBSS) of biotinylated goat anti-mouse IgG H+L 1 hr at 25°C, then washed with PBS for 30 seconds. The sections were then incubated with a 1:50 dilution of exrtravidin HRP for 1 hr at 25° C, then rinsed again with PBS for 30 sec. The reverse sides of the slides were wiped off and cytochemically reacted with 0.05 M 3, 3'-diaminobenzidine tetrahyrochloride containing 0.05% H_2O_2 in 0.05 M TRIS buffer, pH: 7.6 for 1-5 min at 25°C. After final rinsing in PBS, the tissue sections were lightly counter stained with Nissl. We used cerebral cortex and cochlear nucleus tissue sections as positive control material because of their excellent NeuN staining.

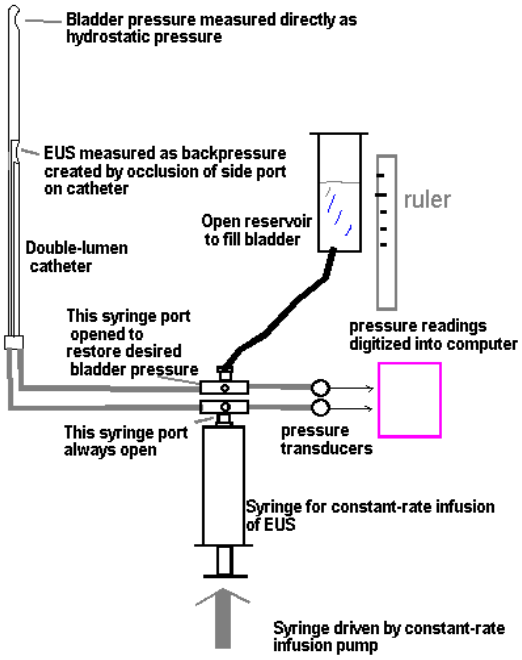

Figure 1

Incubation for Fluoro-Jade B

Fluoro-Jade B is a flourescent cytochemical marker for degenerating cells (Schmued and Hopkins 2000, Krinke et at, 2001, Poirier et al, 2000). The incubation protocol differs from that used for the immunohistochemical stains. The paraffin tissue sections are mounted onto gelatinized slides (or HistoGrip coated slides) and allowed to dry at room temperature. The sections are deparaffinized and rehydrated to 80% ethanol for 5 minutes, then placed into a solution of 80% ethanol containing 1% NaOH for 5 minutes, then into 70% ethanol for 2 minutes and finally washed in distilled water for 2 min. The sections are then placed into an aqueous solution of 0.06% potassium permanganate for 15 minutes, while

agitating gently. They are then washed in distilled water for one minute, and immersed in an aqueous solution of 0.0004% Fluoro-Jade B stain for 20 minutes, while agitating gently. The last step should be performed in the dark, in order to avoid bleaching the Fluoro-Jade B fluorescent stain. Fluoro-Jade B staining solution is prepared from a 0.01% stock solution of Fluoro-Jade B that is made by adding 10 mg of the dye powder to 100 ml of distilled water. To make 100 ml of the staining solution, 4 ml of the stock solution is added to 96 ml of 0.1% acetic acid. The staining solution must be prepared every day, but the stock solution will remain fresh for 2 months if stored at 4/C. After incubation in the staining solution, the slides are washed for one minute in distilled water (repeated 3 times). The slides are then drained on a paper towel and dried on a hotplate at 50/C for 5 minutes and then immersed in xylene for 5 minutes. Finally, they are cover-slipped and allowed to dry.

Histologic sections were photographed using a SPOT Insight digital microscope camera with 1600 x 1200 pixel resolution. Fluoro-Jade B secions wee photographed in the fluorescence mode, with excitation and barrier filters optimized for FITC (fluorescein isothiocyanate).

RESULTS

Measurements of bladder and sphincter pressure

Urodynamic measurements were obtained from cat Sp130 at 41 days, and from cat SP131 at 23 days after implanting the arrays (cat SP131 with the silicon substrate array remains alive, as does SP132. Cat SP132 has yet to be evaluated). We determined the effect of microstimulation in the sacral cord on the hydrostatic pressure within the urinary bladder and on the tone of the urethral sphincter. The cats were anesthetized with Propofol and the urinary

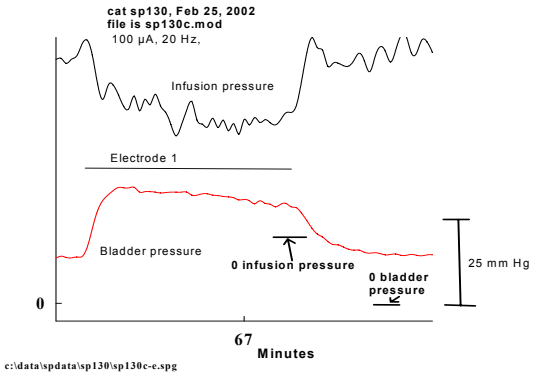

Figure 5A

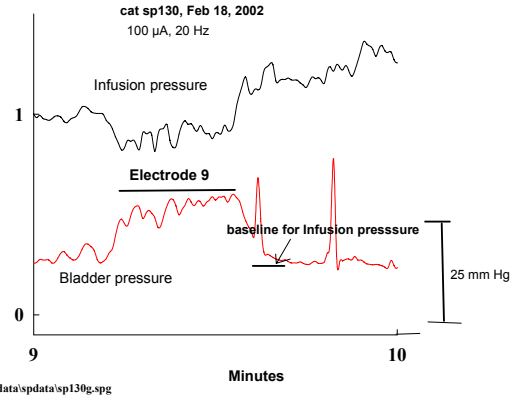

Figure 5B

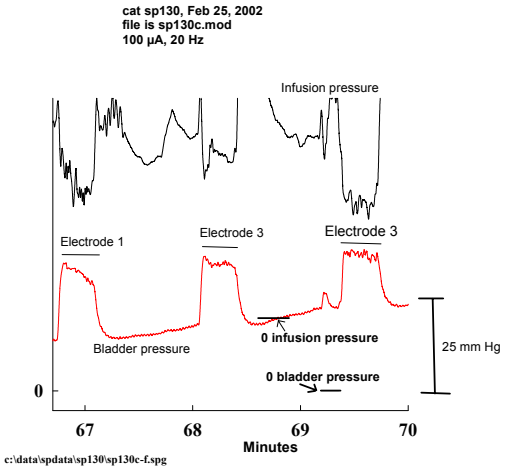

Figure 5C

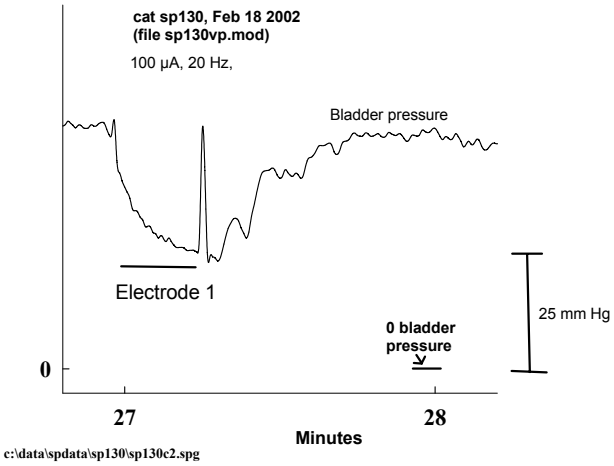

Figure 5D

bladder was catheterized. Hydrostatic pressure within the bladder vesicle was measured with a transducer, using the apparatus depicted in Figure 4, and the data were digitized and stored in a PC computer. The bladder was evacuated, then filled with sterile saline by elevating the open-top reservoir to a height of 20 to 50 cm above the bladder. The constrictive force within the urethral sphincter was measured as an “infusion pressure”; the resistance to the infusion of saline through a port on the side of the catheter as saline was infused continuously at a rate of 100 ml/hr.

Figure 5A shows the hydrostatic pressure within the bladder (lower trace) and the sphincter infusion pressure (upper trace) during stimulation with microelectrode 1 in cat SP130. The tip of this microelectrode was in the intermediolateral cell column at the S_2 level (see Figure 9). In this cat, stimulation through any of electrodes 1, 2 and 3, all of which were in the ILC, induced both relaxation of the sphincter and elevation of bladder pressure (Figure 5C). Although the unilateral stimulation induced only a modest increase in bladder pressure from the baseline

of about 12 mm of Hg, and a modest reduction in the tone of the EUS, pulsing with any one of these electrodes alone was able to induce a weak micturition when the catheter was removed. Electrode 3 induced the greatest relaxation of the urethral sphincter. This is the first animal in which we have been able to reliably elicit both relaxation of the sphincter and elevation of bladder pressure from a single microelectrode. It is interesting that the electrodes in the ILC (electrodes 1,2,3) induced at least as much inhibition of the sphincter as did those closer to the cord's midline (e.g, electrode 9, Figure 5B).

As shown in Figure 5C, the bladder baseline pressure gradually increased between the 66th and 70th minute of the file, probably because some of the saline infused into the sphincter was accumulating within the bladder vesicle. As the baseline pressure increased, the microstimulation caused the bladder pressure to rise to approximately the same endpoint; i.e., the stimulation induced a smaller increase as the baseline pressure increased. Figure 5D shows the effects of stimulation with electrode 1 when the bladder baseline pressure had been elevated to 50 mm of Hg; a very full bladder. In this case, the stimulation induced a marked decrease in bladder pressure as well as complete suppression of spontaneous bladder contractions. This type of "state-dependent" effect may be a consequence of the stimulation having been applied unilaterally in the cord. Although the ability of the microstimulation to suppress spontaneous bladder contractions is potentially useful, the state-dependent effect of the microstimulation is a potential problem when the objective of the stimulation is to induce micturition with a very full bladder.

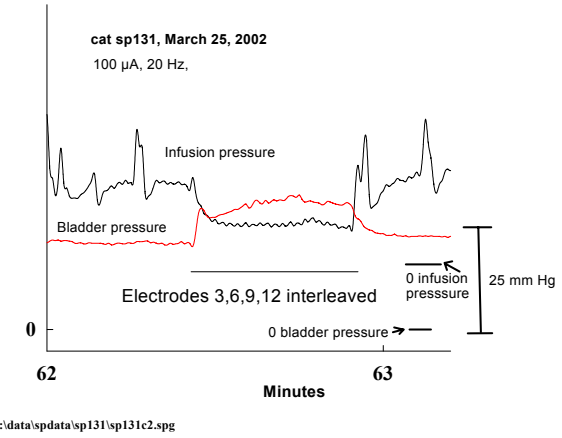

Figure 6

Figure 6 shows the bladder pressure and sphincter infusion pressure recorded from cat SP131, 23 days after implantation of the array of silicon substrate microelectrodes. In this case, interleaved pulsing of electrodes on both sides of the cord induced a modest increase in bladder pressure and a relaxation of the EUS in spite of the rather high bladder baseline pressure (40 mm Hg). Note that the stimulation also inhibited the spontaneous contractions of the sphincter.

Inhibition of spontaneous bladder contractions

Next, the ability of the intraspinal microstimulation to inhibit spontaneous contractions of the bladder was investigated further in cat SP130. The cat was again lightly anesthetized with Propofol. Using an infusion pump, the bladder was slowly filled (2 ml/min) with warm saline until the bladder pressure reached 15-20 mm Hg. At this pressure, the bladder began to exhibit spontaneous hyperreflexia-like contractions. The intraspinal microelectrodes then were pulsed at

various currents and frequencies. Bladder contractions were strongly inhibited by intraspinal microstimulation with microelectrodes located in the intermediate horn of the S_2 spinal cord. The effect was seen even at low baseline bladder pressure. Electrode #9 was very effective (Figure 7). The tip of this electrode was located in the intermediate horn, near the rostral end of S_2 (similar to electrode #8, shown in Figure 10). A wide range of stimulus parameters was

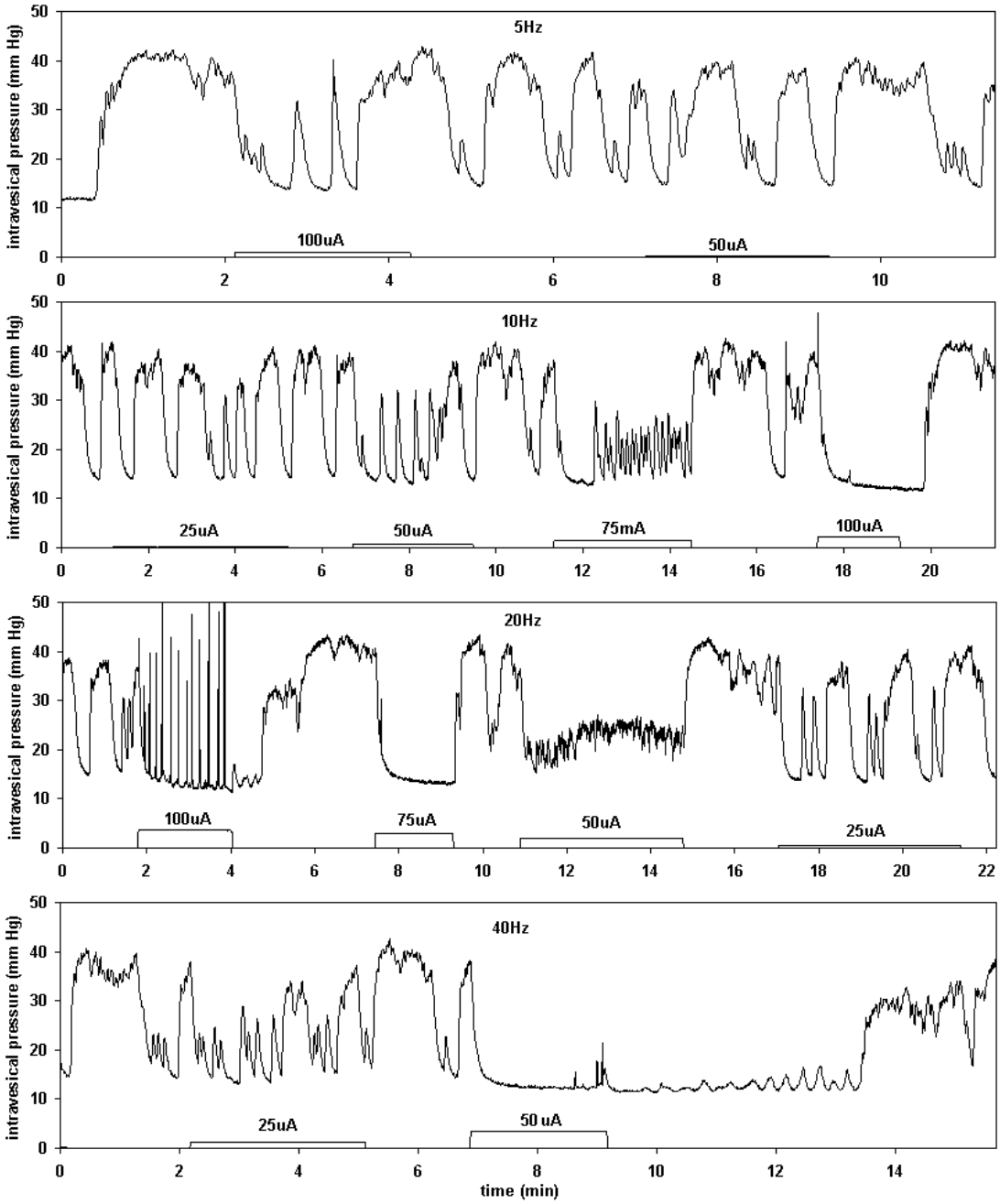

Figure 7

examined, including several minutes of continuous pulsing at up to 50 Hz and at 40 nC/phase. As noted below, this prolonged, high-frequency stimulation apparently induced some tissue injury in

the surrounding tissue, as well as spalling of iridium from the electrode tip. Biphasic cathodic-first pulses of different amplitudes and 400 μsec/phase duration were delivered at frequencies of 5, 10, 20, and 40 Hz. At 5 Hz and a stimulus amplitude of 100 ΜA, there was a partial inhibition of spontaneous bladder activity (top panel). At 10 Hz and 100 ΜA amplitude (2nd panel), a complete inhibition of bladder activity was achieved during a 2 minutes of continuous stimulation. At 20 Hz (3rd panel), a complete inhibition of bladder activity was seen at 75 ΜA amplitude. A stimulus amplitude to 100 ΜA produced spike-like bladder contractions. At 40 Hz and 50 ΜA (bottom panel), a complete inhibition of spontaneous bladder activity was again seen. In addition to bladder inhibition during stimulation, a post-stimulation inhibition of bladder activity approximately 4 minutes in duration was observed. Similar inhibitory post-effects (carryover effects) of stimulation on hyperreflexic bladders were seen in human studies, where electrical or magnetic stimulation of the sacral roots produced a post-stimulus inhibition of bladder hyperreflexia for 1 to 10 minutes (Craggs and McFarlane, 1999; Chartier-Kastler et al., 2001). To our knowledge, the data presented here is the first report of bladder inhibition by intraspinal microstimulation using chronically implanted microelectrodes.

Chronic stimulation protocol

The stimulation regimen for cat SP130 was conducted on the 51st and 52nd day after implantation of the array. The cat was lightly anesthetized with Propofol. Electrodes 1, 3 ,4, 6,7,9 were pulsed for a total of 24 hours (12 hours on each of two successive days), all with the same stimulus parameters. The stimulus waveform was cathodic-first, controlled-current, charge-balanced (biphasic) pulse pairs, 100 ΜA in amplitude and 400 Μs in duration, at 20 Hz per electrode. We used a 10% duty cycle (repeated cycles of 1 minute of stimulation, then 9 minutes without stimulation). This stimulus was administered for 12 hours on each of two successive days.

At the end of the 2nd day of stimulation, the cat was deeply anesthetized with pentobarbital, given i.v. heparin and perfused as described above. The sacral spinal cord was resected and the capsule of connective tissue covering the epoxy array superstructure was removed, leaving the array *in situ.* The array was then withdrawn from the fixed cord. The spinal roots and nerves were identified to determine the exact level of the array. Fixation of the spinal cord was excellent and the electrode array was determined to be on the right side of the cord, near the rostral end of S_2.

NeuN immunostaining and general observations. The position of the array *in situ* is shown in Figure 8. All nine electrode tips were located in the histologic sections, and were shown to be in the right side of the spinal cord. Figure 9 shows the tracks of pulsed electrodes #1, #4 and #7 and Figure 10 shows a section adjacent to the tracks of unpulsed electrodes #2, #5 and #8. Immunohistochemical staining with anti-NeuN antibody highlighted neurons and revealed a reduced NeuN staining of the neurons on the side of the cord into which the array had been implanted. The pattern of NeuN staining was similar around the pulsed (Figures 9, 11,13, 16,18, 20, and 23) and unpulsed electrodes (Figure 10,12,17, 21).

The NeuN-positive sections also revealed variable gliotic scar formations, usually ventral to the tip sites (Figures 11-13, 18 and 20). However, some electrodes (e.g. pulsed electrode #4, Figure 16) were not associated with scars. Neovascularization was observed in association with all electrode capsules (e.g. Figure 11) and there were a few scattered leukocytes near the pulsed and unpulsed electrodes (Figures 13, 17, 21). These were primarily small lymphocytes, and an occasional neutrophil. The tip site of electrode #9 was surrounded by a larger inflammatory lesion approximately 175-200 ：m diameter, that included perivascular cuffs (Figure 23). In Figure 23, we also noted was appeared to be spalled iridium oxide material near the tip of the electrode, which had been pulsed at high amplitude and at high frequency, 12 days before the cat was perfused. Surrounding electrode #9, the perivascular cuffs were composed of lymphocytes and neutrophils, commensurate with our previous observations of inflammatory lesions after regimens of microstimulation in the sacral spinal cord at high amplitude and with a high duty-cycle.

Cytochemical staining with Fluoro-Jade B. Fluorescence microscopy was a used as an adjunct to the NeuN staining. Figure 14 illustrates the appearance of damaged neurons after brain injury (a small stab wound in the cerebral cortex). Only the degenerating neurons fluoresce with the characteristic yellow color. In comparison to this positive control tissue, the neuronal profile near the pulsed electrodes from cat SP130 (Figures 15, 19, 24) or unpulsed electrodes (Figure 22) did not fluoresce and this indicates that the neurons are not degenerating.

DISCUSSION

Collectively, the three stains (Nissl, NeuN, Fluoro-Jade B) showed viable neurons within approximately 50 - 100 ：m of all of the pulsed electrodes, with the exception of electrode #9, which had been subjected to rather prolonged stimulation at high amplitude (40 nC/phase) and high frequency (up to 40 Hz), 12 days prior to the time that the animal was perfused. This tip site was surrounded by a dense aggregate of inflammatory cells approximately 175-200 ：m in diameter, and containing no recognizable neurons. Neurons surrounding the lesion did not fluoresce with the Fluoro-Jade B stain, indicating that they were not degenerating. However, the apparent damage to electrode #9 itself (spalled iridium oxide) and the inflammatory lesion in the surrounding tissue affirms our previous contention that limits must be imposed not only on the stimulus amplitude but also on the pulsing rate and the stimulus duty cycle.

Neurons within approximately 200 ：m of all of the pulsed and unpulsed electrodes stained less darkly for NeuN, and this indicates that their metabolism had been altered by the implantation and/ or the continued presence of the array. Fluoro-Jade B marks neurons that are in an advanced stage of injury, and are actually beginning to degenerate (Poirier et al, 2000). However, the Nissl and NeuN stains revealed intact neurons close to all of the tips except electrode #9, and the absence of any Fluoro-Jade B fluorescence indicates that none of these neurons was degenerating. Overall, there was no discernable difference between the pulsed and unpulsed tip sites, with the exception of electrode #9, as noted above. This speaks well for the safety of the protocol used (1 minute of stimulation at 100 ：A, 400 ：s/phase (40 nC, and 20 Hz, then 9 minutes without stimulation, repeated continuously).

The frequent occurrence of gliotic scars beneath the pulsed and unpulsed electrodes, and also the reduced NeuN staining of neurons within a few hundred microns of the pulsed and unpulsed electrode tips does reveal a limitation of our current electrode configuration an/or our procedure for implanting these electrodes into the spinal cord. These electrodes have been fabricated with blunt tips in order to reduce the risk of microhemorrhages and indeed, we have seen no evidence of these in our series. However, it is possible that the blunt electrodes do contribute to a type of micro-impact trauma in the gray matter of the spinal cord, which contains more large axons and neuropil than the cerebral cortex. In the next quarter, we will be examining tissue from animals in which the electrodes are slightly sharper, and also from the animals implanted with the silicon-substrate arrays. Conversely, the functional significance of the damage caused by the present electrodes configuration should be viewed in the proper perspective; none of the cats has exhibited neurological deficit, and the sacral parasympathetic neuronal machinery remains intact. Also, we have been able to record the action potentials from individual neural units via most of the chronically-implanted iridium microelectrodes, and this confirms our histologic findings that neurons very close to the electrode tips remain functional.

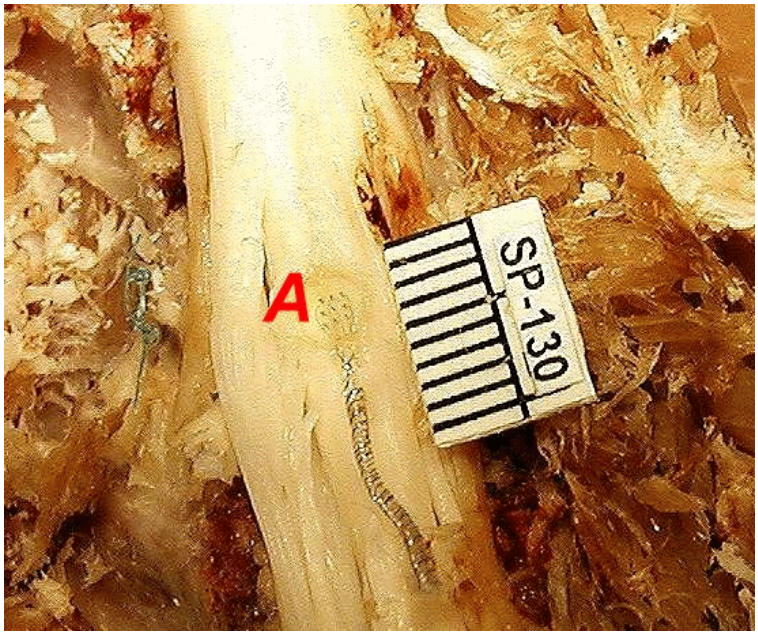

Figure 8. SP130.The dorsal surface of the sacral spinal cord at autopsy shows the top of the 9-electrode array (A) near the junction of the S_1 and S_2 segments. Rule bars = 1 mm.

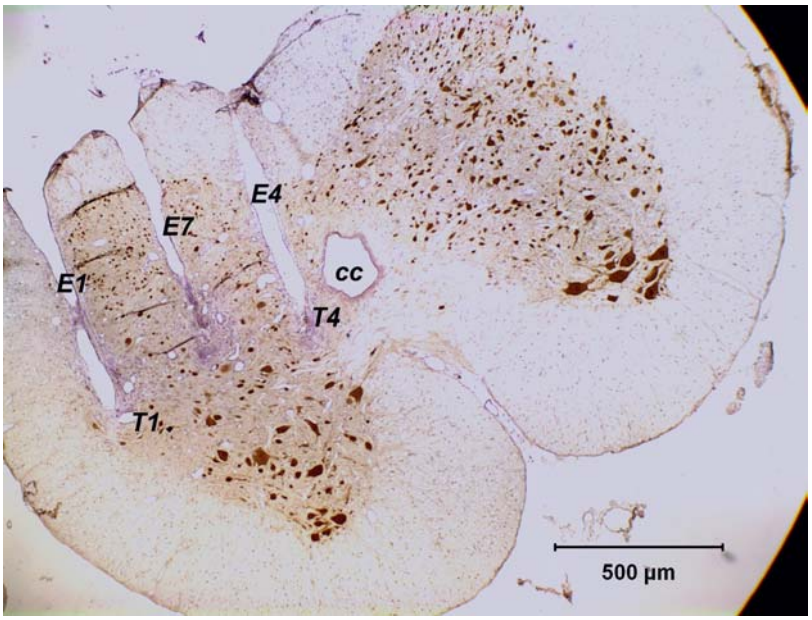

Figure 9. SP130. Panoramic view of a 7 : m section through the sacral cord showing the shafts of three pulsed electrodes, #1, #4, and #7 and the sites of the tips of #1 and #4 (T1, T4). Note the brown NeuN-positive neurons and their processes on both sides of the cord. Note the reduced density of the NeuN staining around the electrode shafts and tip sites. The central canal (CC) is also shown. NeuN stain with Nissl counter stain.

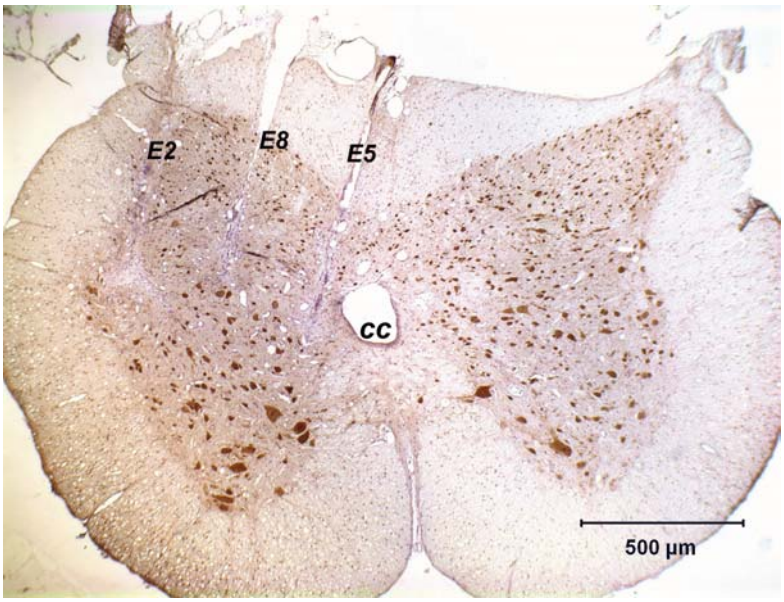

Figure 10. A panoramic view of a 7 ：m section through the sacral cord, and through part of the shafts of three unpulsed electrodes, #2, #5, and #8. Note the reduction in the density of the brown NeuN staining of the neurons and their processes in the vicinity of the electrode tips . The central canal (CC) is also shown. NeuN stain with Nissl counter stain.

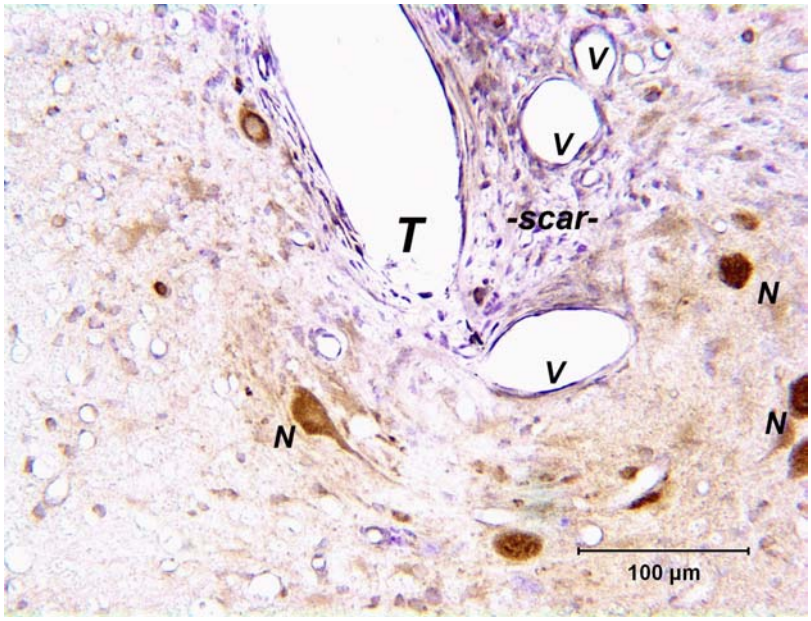

Figure 11. Higher magnification of a portion of the capsule surrounding the shaft of pulsed electrode #1 (also shown in Figure 9). The electrode tip site (T) is surrounded by several NeuN-positive neurons (N), within 150 ：m of the electrode tip. A glial scar is to the right of the tip site. Note several blood vessels (v) within the scar. NeuN stain with Nissl counter stain.

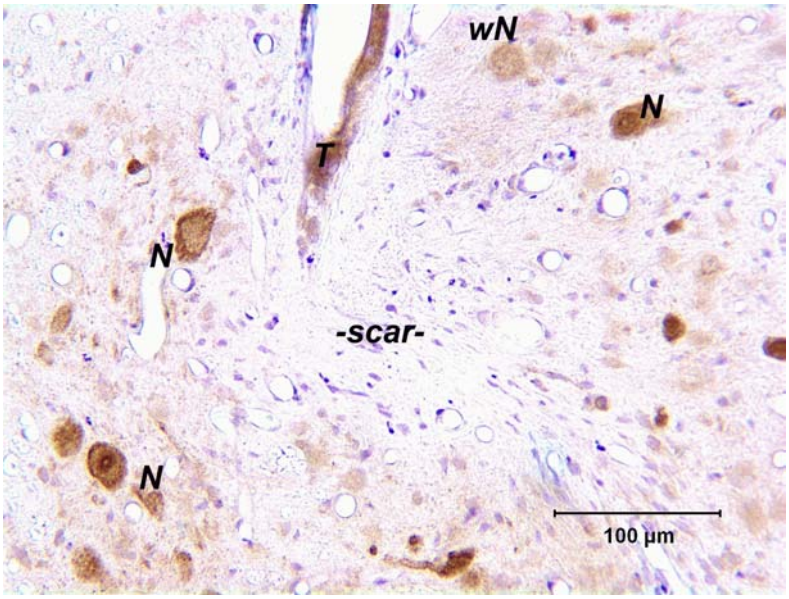

Figure 12. High magnification view the tip site (T) and a portion of the capsule surrounding the shaft of unpulsed electrode #2. Note two NeuN-positive neurons (N) within 150 ：m of the electrode tip, and several others more distant from the tip. Note that some of the NeuN-positive neurons are stained only weakly (wN). An elongated gliotic scar lies ventral to the tip site. NeuN stain with Nissl counter stain.

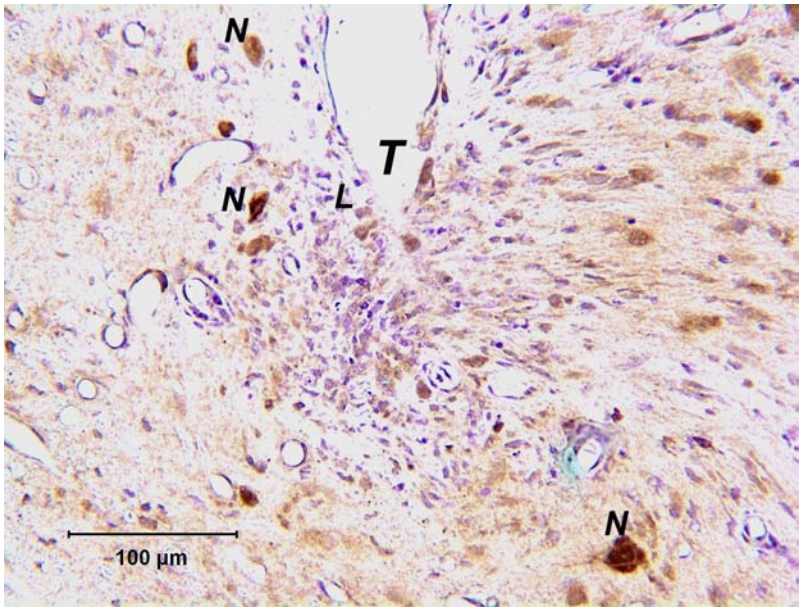

Figure 13. High magnification view of the tip site (T) of pulsed electrode #3. Note the darkly stained NeuN-positive neurons (N) and the weaker NeuN staining of the neurons to the right of the tip site. A few leukocytes (L) are mixed with astroglial cells ventral to the tip site. NeuN stain with Nissl counter stain.

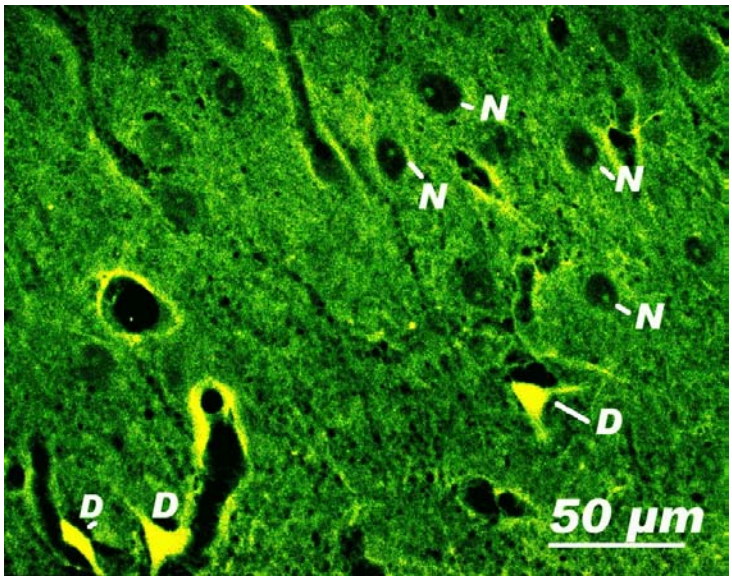

Figure 14. A micrograph from a section stained with the fluorochrome Fluoro-Jade B. The section of cat cerebral cortex is adjacent to a small stab wound made 4 hours prior to perfusion. Damaged neurons (D) fluoresce yellow against the green neuropil, while undamaged neurons (N) appear darker than the neuropil. Fluorescent microscopic image without counter stain.

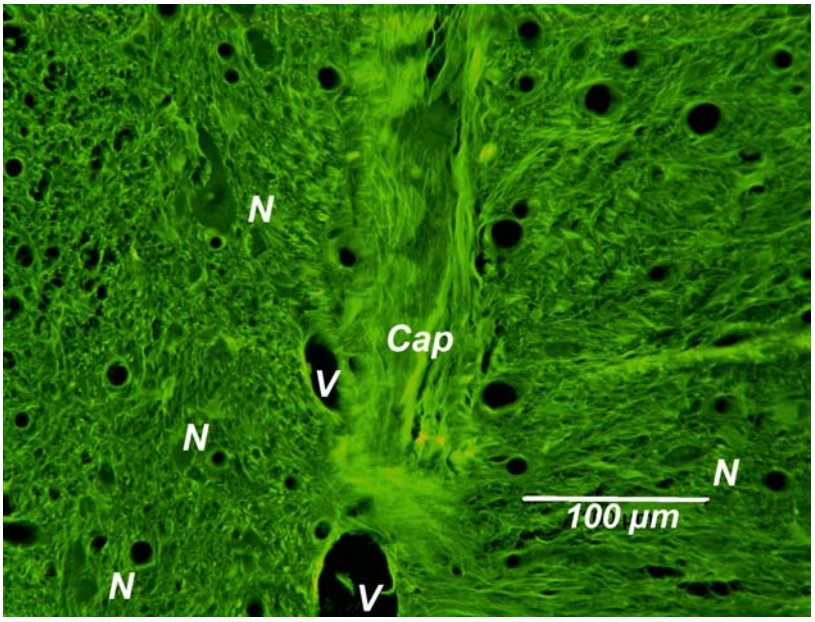

Figure 15. A micrograph from a section stained with the fluorochrome Fluoro-Jade B. This is a section 14-21 : m rostral to the section shown in Figure 13 and the actual tip site, and is just grazing the capsule (Cap) surrounding the electrode track of pulsed electrode #3. Several neurons and their processes (N) appear darker than the neuropil, in contrast to the degenerating neurons in Figure 14, and therefore they are presumed not to be degenerating. Fluorescent microscopic image without counter stain.

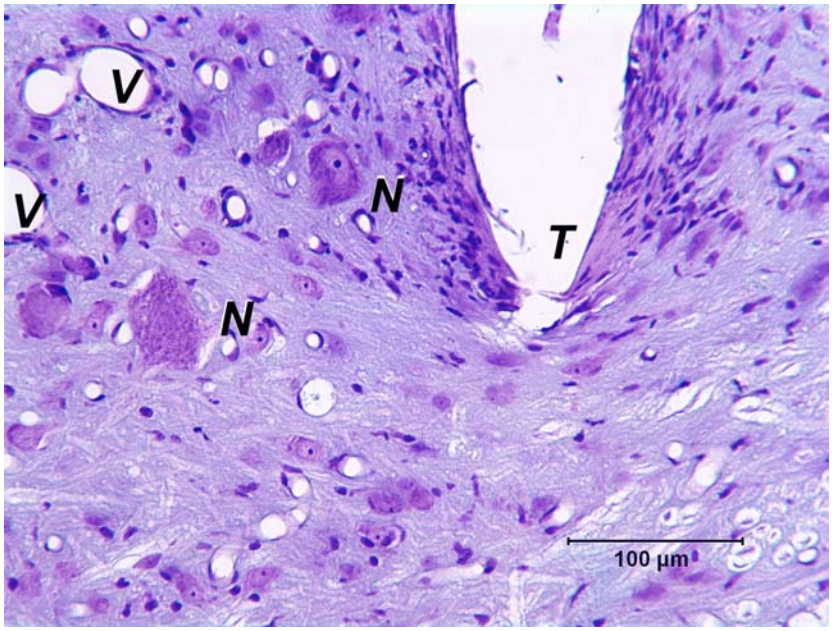

Figure 16. High magnification view of the tip sit site of pulsed electrode #4. Note the electrode tip site (T) and normal-appearing neurons (N) within 100 ：m of the tip. Several small blood vessels (v) are also shown. Nissl stain.

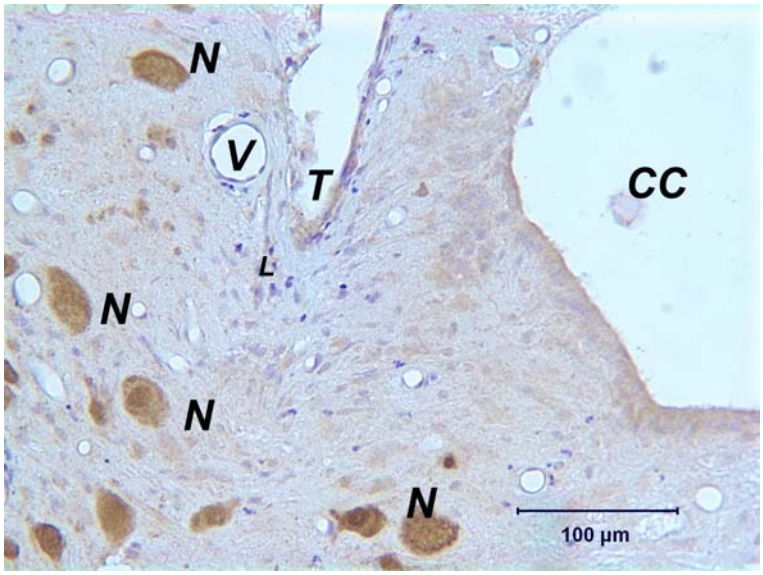

Figure 17. High magnification of the tip site (T) of unpulsed electrode #5. Note the NeuN-positive neurons (N) within 150 ：m of the tip, a few scattered leukocytes (L) near the electrode tip, and a blood vessel (v) adjacent to the electrode shaft. The spinal cord's central canal (CC) is also shown. NeuN stain with Nissl counter stain.

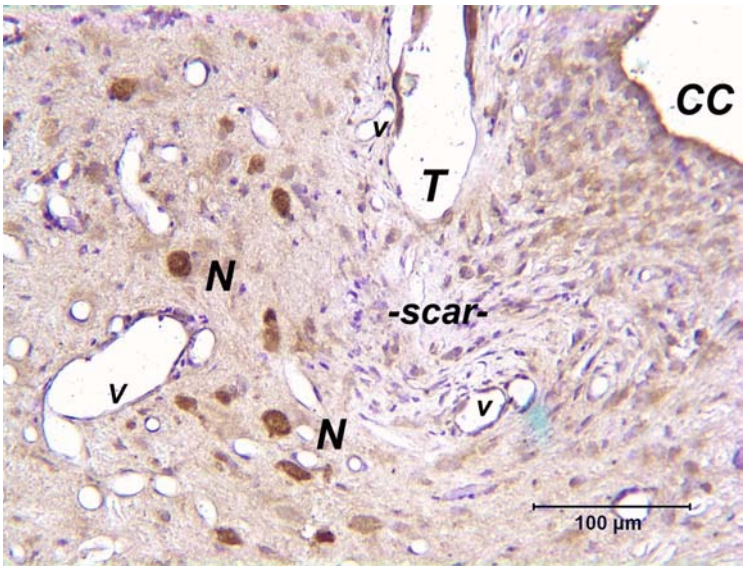

Figure 18. The tip site (T) of pulsed electrode #6. Note the NeuN-positive neurons (N) within 150 ：m of the tip, and a gliotic scar ventral to the electrode tip. The central canal (CC) is also shown at upper right. NeuN stain with Nissl counter stain.

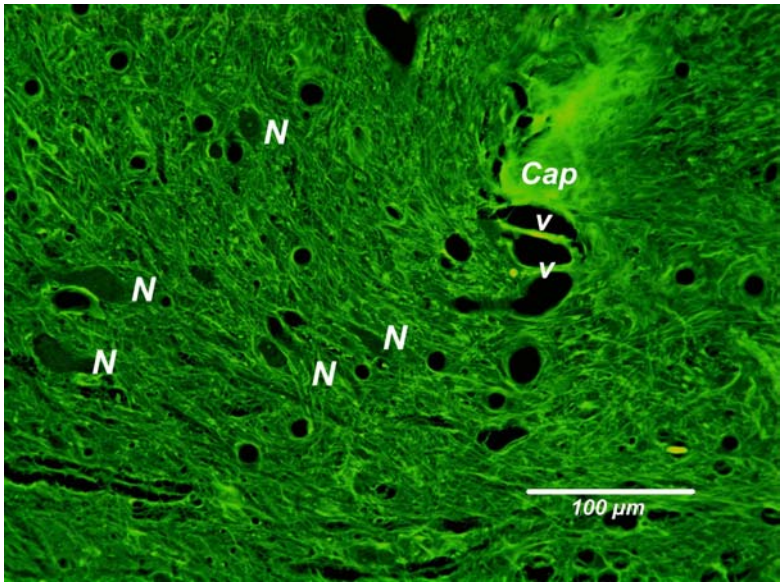

Figure 19. A micrograph of a section through the capsule (Cap) surrounding pulsed electrode #6. This section is approximately 14-21 ：m rostral to the section shown in Figure 18. Neurons (N) do not fluoresce and thus do not appear to be damaged. Blood vessels (v) and several normal neurons (N) are also shown. Fluoro-Jade B stain without counter stain.

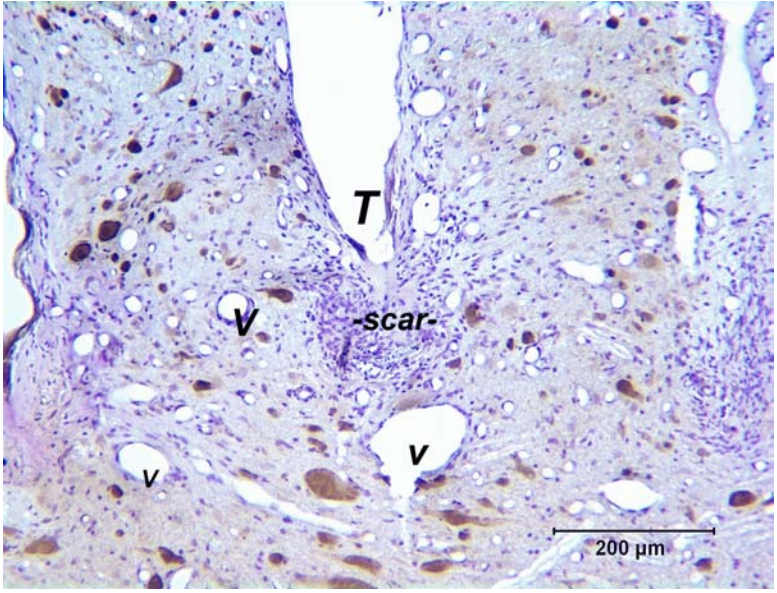

Figure 20. The tip site (T) of pulsed electrode #7. Note several brown-stained NeuN-positive neurons within 150 ：m of the electrode tip. A glial scar approximately 125 ：m in diameter is ventral to the electrode tip. NeuN stain with Nissl counter stain.

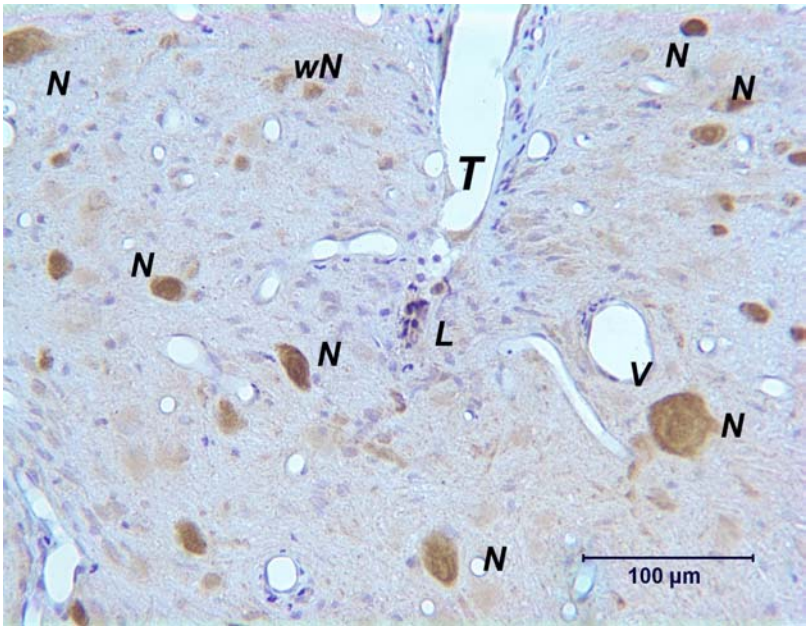

Figure 21. The tip site (T) of unpulsed electrode #8. Note several NeuN-positive neurons (N) within 150 ：m of the electrode tip, scattered blood vessels (v) and a few leukocytes ventral to the electrode tip (L). Neurons closer to the tip of this unpulsed electrode are stained less intensely. NeuN stain with Nissl counter stain.

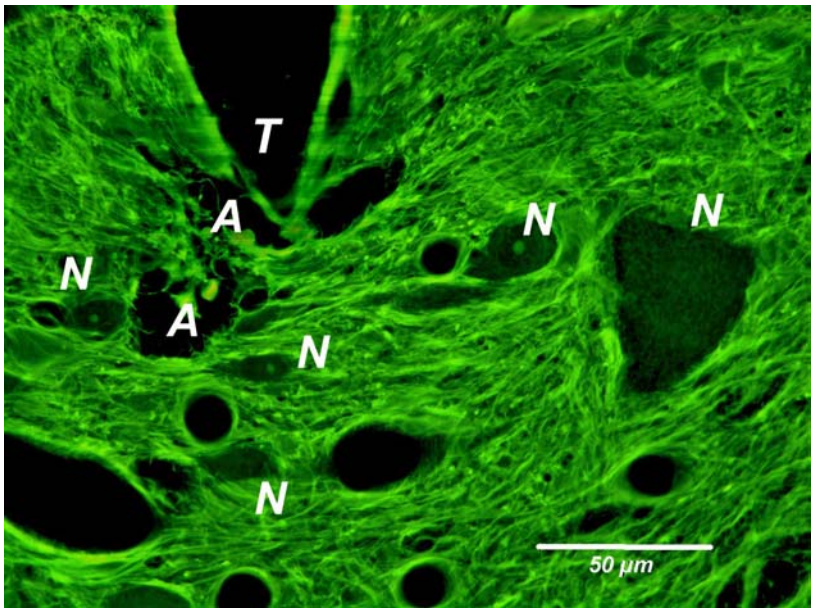

Figure 22. The tip site (T) of unpulsed electrode #8. Nearby neurons (N) are do not fluoresce and thus do not appear to be degenerating. Blood vessels (v) and a cutting artifact (A) are shown. Fluoro-Jade B without counter stain.

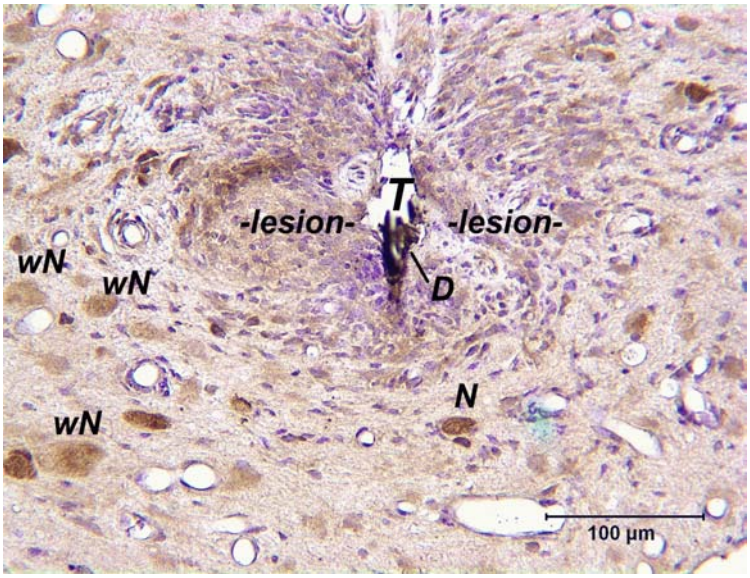

Figure 23. The tip site (T) of electrode # 9 that was pulsed with high amplitude and at high frequency. The tip site is surrounded by a large inflammatory lesion. The tip site contains a deposit of dense material (D), probably iridium oxide spalled from the electrode tip. Note the normal-appearing neurons (N) and the more weakly-stained neurons (wN) closer to the tip site. NeuN stain with Nissl counter stain.

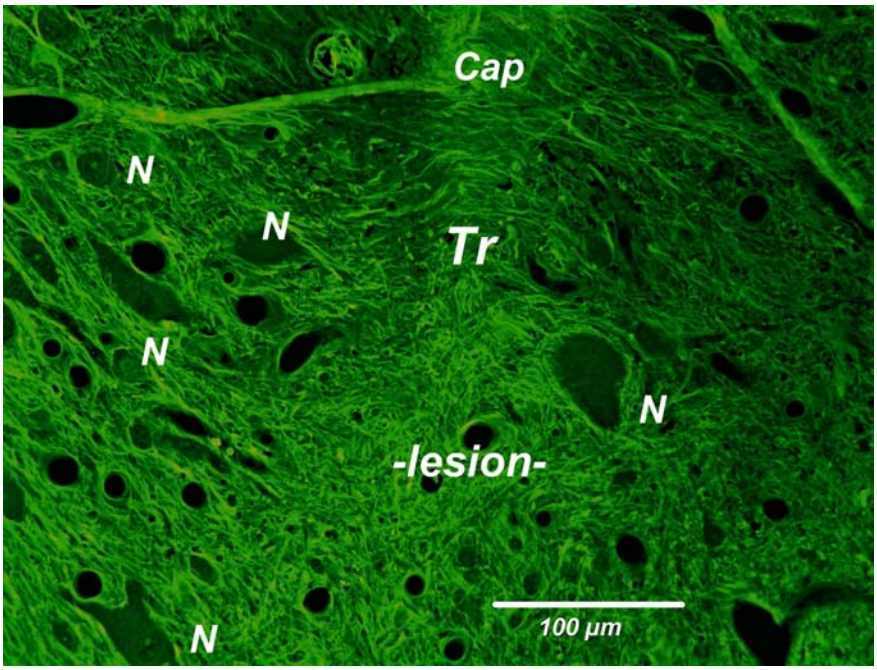

Figure 24. A micrograph from a section approximately 35 ：m rostral to the tract and tip site of pulsed electrode #9. The capsule (Cap) surrounding the electrode track is visible. The lesions surrounding the tip site is devoid of recognizable neurons but those adjacent to the lesion are not degenerating. Blood vessels (v) and several non-fluorescent neurons (N) are also shown. Fluorescent microscopic image without counter stain.

REFERENCES

1. Chartier-Kastler, E. J., J. L. Ruud Bosch, M. Perrigot, M. B. Chancellor, F. Richard, and P. Denys. Long-term results of sacral nerve stimulation (S3) for the treatment of neurogenic refractory urge incontinence related to detrusor hyperreflexia. J Urol 164: 1476-80., 2000.

2. Chartier-Kastler, E. J., P. Denys, M. B. Chancellor, A. Haertig, B. Bussel, and F. Richard. Urodynamic monitoring during percutaneous sacral nerve neurostimulation in patients with neurogenic detrusor hyperreflexia. Neurourol Urodyn 20: 61-71, 2001.

3. Craggs, M., and J. McFarlane. Neuromodulation of the lower urinary tract. Exp Physiol 84: 149-60., 1999.

4. Krinke, G. J., W. Classen, N. Vidotto, E. Suter, and C. H. Wurmlin. Detecting necrotic neurons with fluoro-jade stain. Exp Toxicol Pathol 53: 365-72., 2001.

5. Poirier, J. L., R. Capek, and Y. De Koninck. Differential progression of Dark Neuron and Fluoro-Jade labelling in the rat hippocampus following pilocarpine-induced status epilepticus. Neuroscience 97: 59-68, 2000.

6. Schmued, L. C., and K. J. Hopkins. Fluoro-Jade B: a high affinity fluorescent marker for the localization of neuronal degeneration. Brain Res 874: 123-30., 2000.